blood®
Regular Article

LYMPHOID NEOPLASIA

RhoA G17V is sufficient to induce autoimmunity and promotes T-cell lymphomagenesis in mice

Samuel Y. Ng,[1] Leon Brown,[1] Kristen Stevenson,[2] Tiffany deSouza,[1] Jon C. Aster,[3] Abner Louissaint Jr,[4] and David M. Weinstock[1,5]

[1]Department of Medical Oncology and [2]Department of Biostatistics and Computational Biology, Dana-Farber Cancer Institute, Harvard Medical School, Boston, MA; [3]Department of Pathology, Brigham and Women's Hospital, Boston, MA; [4]Department of Pathology, Massachusetts General Hospital, Boston, MA; and [5]Broad Institute of MIT and Harvard University, Cambridge, MA

KEY POINTS

- Expression of RhoA G17V in CD4$^+$ cells results in cellular and humoral autoimmunity.
- RhoA G17V expression with *Tet2* loss induces T-cell lymphomas with features of AITL.

Patients with angioimmunoblastic T-cell lymphoma (AITL) and other peripheral T-cell lymphomas that harbor features of follicular helper T (T_{FH}) cells have a very poor prognosis. These lymphomas commonly present with paraneoplastic autoimmunity and lymphopenia. RhoA G17V mutation is present in 60% of T_{FH}-like lymphomas, but its role in tumorigenesis is poorly understood. We generated transgenic mice that express RhoA G17V under the control of murine CD4 regulatory elements at levels comparable to a heterozygous mutation (tgRhoA mice). These mice had markedly reduced naive T cells but relatively increased T_{FH}-cell populations. Surprisingly, naive CD4 T cells expressing RhoA G17V were hyperreactive to T-cell receptor stimulation. All tgRhoA mice developed autoimmunity that included a cellular infiltrate within ears and tails that was recapitulated in wild-type (WT) recipients after bone marrow transplantation. Older tgRhoA mice developed elevated serum titers of anti-double-stranded DNA antibodies and renal immune complex deposition. RhoA G17V mice crossed with *Tet2*$^{fl/fl}$; Vav-Cre$^+$ mice, which delete *Tet2* throughout the hematopoietic compartment, developed T-cell lymphomas that retained histologic and immunophenotypic features of AITL and had transcriptional signatures enriched for mechanistic target of rapamycin (mTOR)-associated genes. Transplanted tumors were responsive to the mTOR inhibitor everolimus, providing a possible strategy for targeting RhoA G17V. Taken together, these data indicate that RhoA G17V contributes to both neoplastic and paraneoplastic phenotypes similar to those observed in patients with T_{FH} lymphomas. (*Blood*. 2018;132(9):935-947)

Introduction

A subset of peripheral T-cell lymphomas (PTCLs) have features of follicular helper T (T_{FH}) cells.[1] These lymphomas, which share both immunophenotypes and transcriptional profiles with T_{FH} cells, include angioimmunoblastic T-cell lymphoma (AITL) and a subset of PTCL-not otherwise specified.[2-4]

T_{FH} cells are an effector T-cell subtype that enable B-cell proliferation, differentiation, somatic hypermutation, isotype switching, and plasma cell differentiation in germinal centers.[5] T_{FH} cells are marked by CXCR5 and PD-1 coexpression[6,7] and express inducible T-cell costimulator (ICOS).[8] Recent data have implicated the mTORc1 and mTORc2 complexes in T_{FH} cell differentiation and function, although conflicting results indicate that these functions are likely to be context-specific.[9,10]

T_{FH} lymphomas are strongly associated with autoimmune phenomena, including rashes, hypergammaglobulinemia, and cytopenias.[2,3] Only 20% to 30% of these lymphomas are cured, so better treatments are desperately needed.[2] Recent studies of the mutational landscape of PTCL samples have demonstrated that up to 80% of T_{FH}-like lymphomas have loss-of-function mutations in the methylcytosine dioxygenase TET2 that are frequently biallelic,[11,12] and approximately 60% have G17V substitutions in the small GTPase RhoA.[13-15]

RhoA is important for multiple T-cell functions, including cell polarization and migration, immune synapse formation, and modulation of T-cell receptor (TCR) signaling.[16] The RhoA G17V substitution is highly specific for T_{FH}-like lymphomas and is typically heterozygous.[13-15] RhoA G17V fails to bind GTP and sequesters guanine-nucleotide exchange factors,[13-15] suggesting a dominant-negative activity on Rho/Rac/Cdc42 or other GTPase signaling that would differ from complete loss of RhoA function.

Zang et al.[17] recently overexpressed RhoA G17V in peripheral CD4$^+$ T cells and then adoptively transferred them into TCRα-deficient mice, reconstituting the T-cell compartment. In this system, lentiviral transduction of RhoA G17V into wild-type (WT) CD4$^+$ T cells followed by adoptive transfer did not result in skewing of peripheral compartments toward T_{FH} cells, autoimmunity, or T-cell tumors. In contrast, transduction of RhoA G17V into *Tet2*$^{-/-}$ CD4$^+$ T cells and adoptive transfer led to lethal autoimmunity.

We sought to determine the effects of expression of RhoA G17V at levels consistent with heterozygous mutation in a system that does not require adoptive transfer and in vivo expansion. We show that this approach leads to a reduction in peripheral naive T cells and fully penetrant autoimmunity in mice expressing RhoA G17V under CD4 control. When crossed with mice that lack Tet2, RhoA G17V expression promotes the development of mature T-cell lymphomas that are highly reminiscent of human T_{FH}-like lymphomas.

Materials and methods

Mice

The transgenic mouse construct was generated by insertion of the human *RHOA* G17V-mutated coding sequence into the mCD4 e/p Sal-(hCD2) plasmid,[18] a gift from Dan Littman (Addgene plasmid #24070). Transgenic mice Tg(Cd4-RHOA^{G17V})DWsk were generated through injection of DNA into fertilized C57Bl/6 zygotes, followed by implantation into pseudopregnant females. We report mice derived from a founder with 1 to 2 copies integrated, as determined by quantitative polymerase chain reaction (qPCR), with the proposed transgene designation Tg(Cd4-RHOA^{G17V})2DWsk.

Flow cytometry

Flow cytometry was performed on single-cell suspensions of thymus, spleen, lymph nodes, or tail skin as indicated, using monoclonal antibodies against the noted antigens. Antibody clone names are available in supplemental Methods, available on the *Blood* Web site. Analysis was performed using either a BD Biosciences FACSCanto or LSRFortessa. Flow sorting for mixed leukocyte reactions and transcriptomic analysis was performed using a BD Biosciences FACSARIA. Intracellular staining was performed with the Foxp3/Transcription Factor Staining Buffer set (Thermo Fisher) or IC Fixation Buffer (Thermo Fisher) in combination with methanol. Tail skin was harvested for flow cytometry, as previously described.[19]

Mouse immunizations

Mice included in the tumor cohorts were intraperitoneally injected with a mixture of 100 μg NP40-Ovalbumin (Santa Cruz) with 50% Alum (Thermo Scientific) in 100 μL total volume. For tumor induction, mice were injected monthly to a maximum of 7 injections.

Everolimus treatment

After adoptive transfer of tumor cells, mice were dosed daily with 10 mg/kg Everolimus (Selleck Chemicals) or 10% dimethyl sulfoxide in phosphate-buffered saline by oral gavage for the durations indicated. Mice were euthanized when they met Institutional Animal Care and Use Committee criteria (eg, weight loss, hind limb paralysis). For pharmacodynamic analysis, 14 days after injection of 500 000 tumor cells, mice were dosed for 5 days with 10 mg/kg daily with everolimus or vehicle and were euthanized 2 hours after the final dose.

Statistical analysis

Comparison of continuous measures between 2 groups was made using a 2-sided Welch's *t* test and were considered significant at the $<.05$ level. Comparison of cells expressing CD25 and CD69 between tgRhoA-naive and WT T cells, and ovalbumin (OVA) peptide and phorbol 12-myristate 13-acetate (PMA)-ionomycin were assessed using a 2-way analysis of variance with a Tukey correction for multiple comparisons. A repeated measures analysis of variance was used to the test for a difference in immunoglobulin G (IgG) antibody deposition in the glomeruli of the mice between WT and tgRhoA based on 7 to 8 sections per mouse. Differential expression between experimental criteria was determined using raw counts and normalization procedures within the DESeq2 package in R, based on a negative binomial distribution. Unsupervised clustering was performed using the Euclidean distance with complete linkage method in the R package pheatmap, and principal component analysis was performed on the top 1000 most variable genes, as determined using the rlog transformation function within the DESeq2 package to stabilize the variance. For better cluster visualization, the range of colors was rescaled to −4 to 4 in increments of 0.5, using breaks option within the pheatmap package. The false-discovery rate (FDR) by the Benjamini and Hochberg method was used to adjust for multiple comparisons. The ordered lists determined by differential expression were then used in gene set enrichment analysis (GSEA; Broad Institute), and the FDR *q* values were reported. Overall survival was measured as the time from birth to the time of death calculated using the method of Kaplan and Meier, and curves were compared using a 2-sided log-rank test and considered significant at the $<.05$ level.

Results

T-cell lymphopenia in CD4-RhoA G17V mice

We generated transgenic mice that express human *RHOA* G17V transcript driven by elements from the murine *Cd4* locus,[18] with the resultant strain Tg(Cd4-RHOA^{G17V})2DWsk hereafter referred to as tgRhoA mice (Figure 1A). Mice harboring the transgene were born in expected Mendelian ratios. We selected a founder line with 1 to 2 copies of the transgene based on qPCR of genomic DNA (Figure 1B). Probe-based qPCR of cDNA from CD4$^+$ cells purified from lymph nodes indicated that the transgene transcript was expressed at approximately 60% of endogenous RhoA transcript levels (Figure 1C). Immunoblotting with a human and mouse cross-reactive RhoA antibody demonstrated no substantial differences in RhoA protein expression from whole thymocytes (Figure 1D).

According to the transgene expression construct, RhoA G17V expression should begin in the CD4$^+$CD8$^+$ double-positive stage of T-cell development.[18] Analysis of thymic T cells from 6- to 10-week old tgRhoA mice showed increased CD4$^+$CD8$^+$ (double-positive) T cells and decreased CD4$^+$CD8$^-$ and CD8$^+$CD4$^-$ (single-positive) T cells compared with WT littermate controls (Figure 1E). Thymic development can also be monitored on the basis of the surface expression of TCRβ and CD69.[20] Cells first express surface CD69 alone and then express TCRβ with CD69, and then downregulate CD69. Analysis of tgRhoA thymocytes indicated a defect in development from the CD69 single-positive to the CD69/TCRβ double-positive stage (supplemental Figure 1A-B). According to previous studies,[20] this indicates that tgRhoA CD4$^+$CD8$^+$ thymocytes develop at least through the initial stages of positive selection. Of the tgRhoA cells that were TCRβ$^+$, there was a significant increase in the percentage that expressed PD-1 (supplemental Figure 1B).

The defects in T-cell development were associated with decreases in splenic CD4$^+$ and CD8$^+$ T cells compared with those

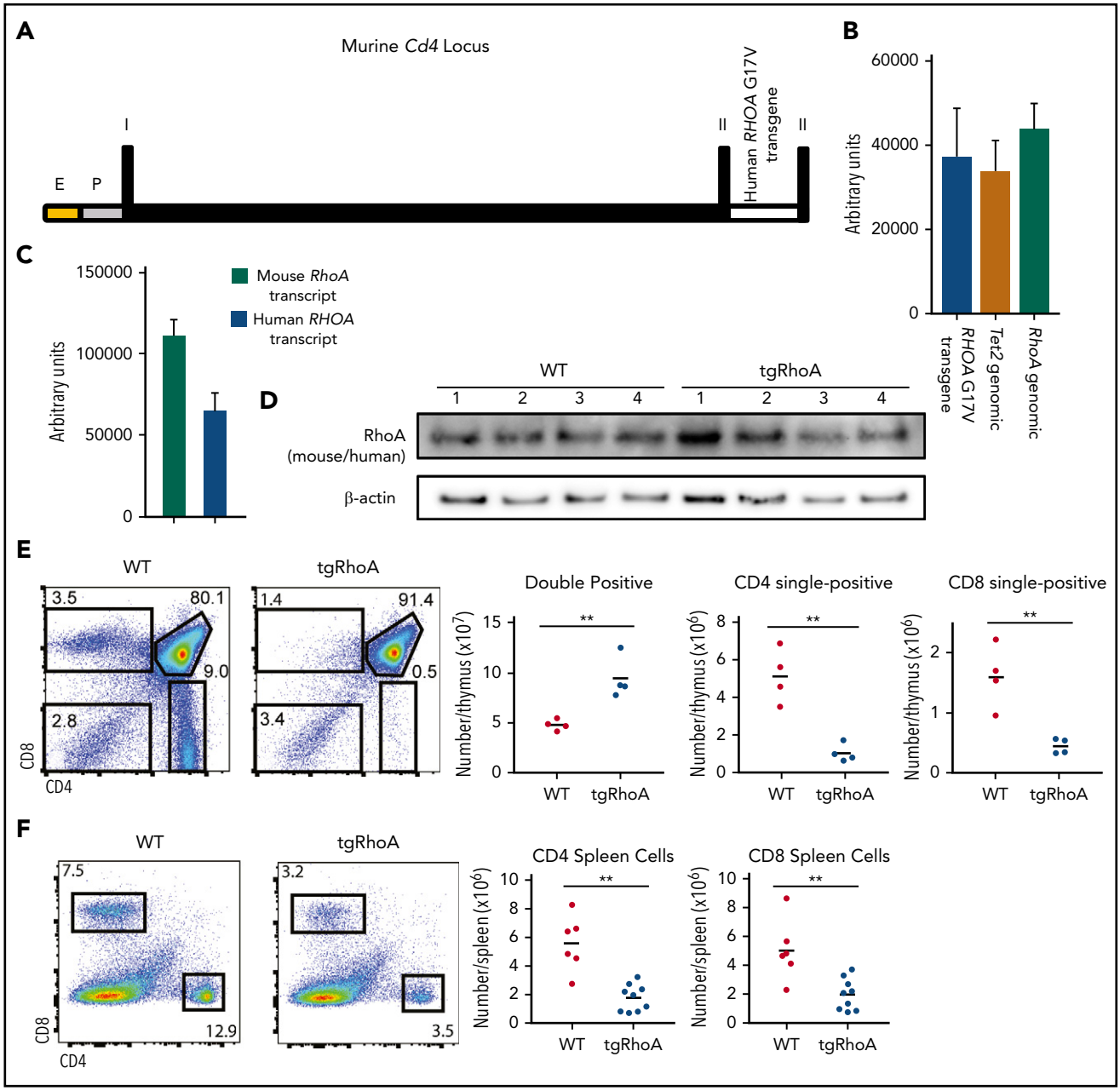

Figure 1. Generation of Cd4-RHOA^{G17V} transgenic mice. (A) Schematic representation of the transgene construct, which includes the murine *Cd4* minimal enhancer fused to the human *CD4* minimal promoter followed by the murine *Cd4* exon 1, which consists of 5′ UTR, intron 1, and exon 2, with the human RHOA transgene inserted 5′ to the endogenous ATG. E, murine *Cd4* minimal enhancer; P, human *CD4* minimal promoter; I, exon 1; II, exon 2. (B) Quantitative PCR of genomic DNA from mouse tail DNA was performed using SYBR green analysis of the *RHOA* transgene compared with endogenous *Tet2* ($P = .6953$) or *RhoA* ($P = .4444$). (C) Quantitative PCR of transcripts from tgRhoA CD4$^+$ lymph node cells using amplification and probe-based detection of sequences specific for mouse or human *RhoA* (112 253 vs 64 819; $P = .0006$). (D) Immunoblot analysis of whole thymus extracts from tgRhoA or control littermates. Each lane represents whole thymic extracts from a single WT or tgRhoA mouse. The RhoA antibody cross-reacts with human and mouse proteins, which have equivalent molecular weights. (E) Flow cytometric evaluation of tgRhoA or control littermate thymuses. Data are representative of 3 independent experiments. (F) Flow cytometric analysis of splenic CD4$^+$ and CD8$^+$ cells of tgRhoA and control littermates. Data are representative of 3 independent experiments. All *P* values calculated by *t* test with Welch's correction.

from WT littermates (Figure 1F). Taken together, this indicates that expression of RhoA G17V during thymic development is sufficient to impair the double-positive to single-positive T-cell transition and to reduce peripheral T-cell numbers.

Autoimmunity from RhoA G17V expression

Between 8 and 10 weeks after birth, 100% of tgRhoA mice developed a striking phenotype of dermatitis, soft tissue inflammation, and then fibrosis that first involved the ears and tails (Figure 2A), followed by progression to hair-covered skin. Immunohistochemistry identified a mixed-cellular infiltrate of polymorphonuclear and CD4$^+$ T cells within involved areas that extended from skin into underlying connective tissue and muscle (Figure 2A). To determine the cellular composition of the infiltrate, tail skin from 10-week old mice was dissociated to recover hematopoietic cells.[19] There were significantly increased percentages of CD4$^+$TCRβ$^+$ T cells and CD11b$^+$Ly-6G$^+$ myeloid cells recovered from tgRhoA mice compared with hematopoietic

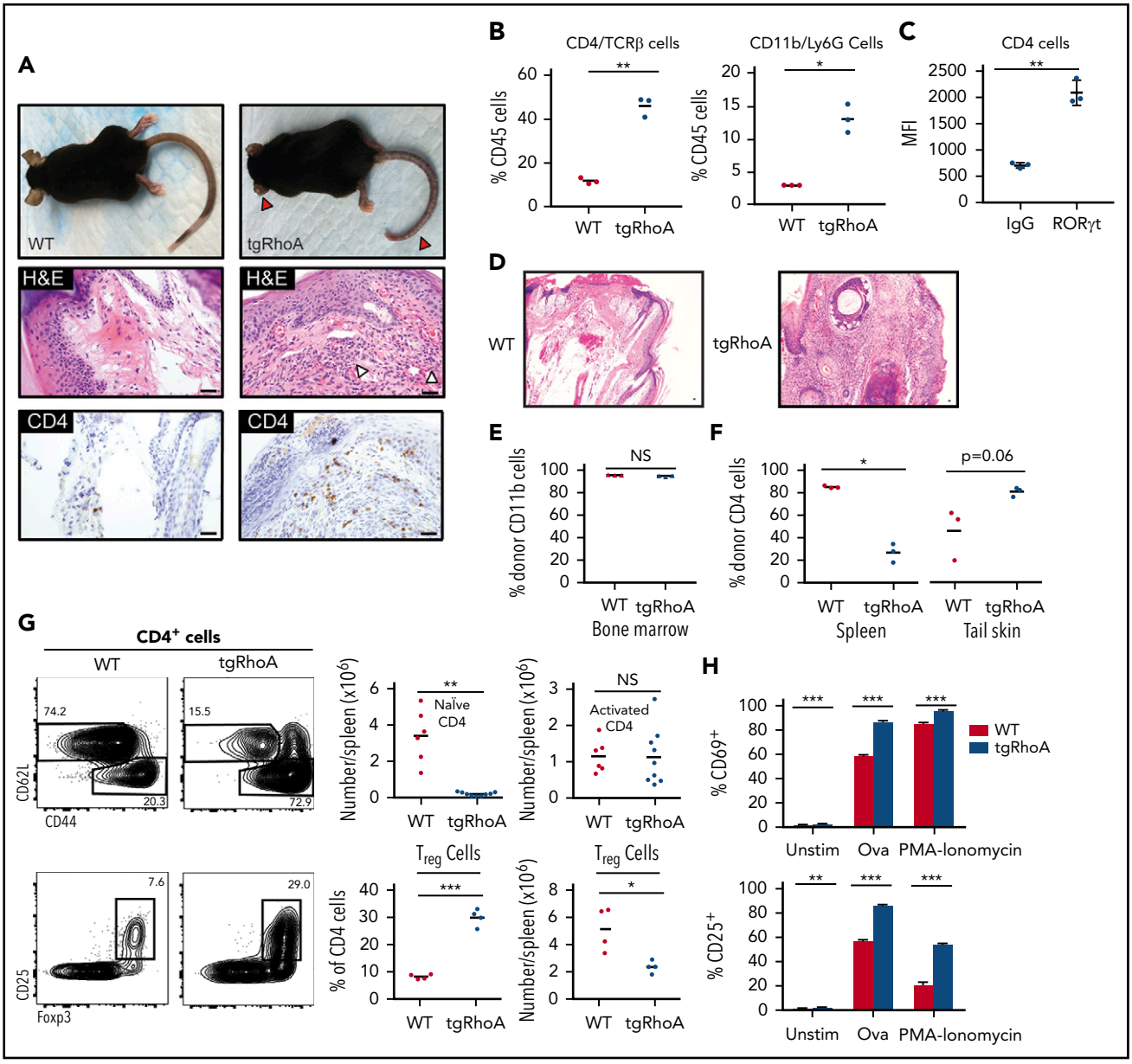

Figure 2. TgRhoA mice develop hematopoietic cell-dependent autoimmunity. (A) Gross findings demonstrating fibrosis of ears and tail (red arrowheads) of mice from the indicated genotypes (top). Hematoxylin and eosin (H&E) staining of mouse tail tips demonstrating a polymorphonuclear cell infiltrate (white arrowheads) and immunohistochemistry of CD4-positive cells (bottom). Scale bars, 100 μm. (B) Percentage of CD4/TCRβ and CD11b/Ly6G cells among CD45$^+$ hematopoietic cells recovered from tail skin. (C) Mean fluorescence intensity of RORγt expression in tgRhoA CD4$^+$ cells compared with isotype control ($P = .0076$). (D) H&E staining of tail tips from congenic recipient mice 10 weeks after injection with WT or tgRhoA bone marrow. Scale bars, 100 μm. (E) Flow cytometric analysis of bone marrow donor (CD45.1$^-$) CD11b$^+$ cells. (F) Flow cytometric analysis of bone marrow donor (CD45.1$^-$) CD4$^+$ cells in spleen or recovered from tail skin. (G) Representative flow cytometric profiles of splenic CD4$^+$ naive and activated (top) or T_{reg} populations (bottom) along with quantification. Plots and graphs are representative of 3 experiments. (H) Expression of activation markers from sorted CD4$^+$CD62L$^+$CD44$^-$CD25$^-$-naive T cells 48 hours after mixed leukocyte reaction of tgRhoA-OT-II or WT-OT-II T cells unstimulated, stimulated with 5 μg/mL $OVA_{323-339}$ peptide, or stimulated with PMA/Ionomycin. Data are representative of 2 independent experiments. All *P* values calculated by *t* test with Welch's correction.

cells within tails from their WT littermates (Figure 2B; supplemental Figure 2A-B). The morphologic and immunophenotypic characteristics of these tails were suggestive of a T_H17-type inflammatory infiltrate. In fact, CD4$^+$ T cells infiltrating the tail dermis expressed RORγt, the lineage-defining transcription factor for T_H17 cells[21] (Figure 2C; supplemental Figure 2C).

To confirm that this autoimmune phenotype was a result of defects in hematopoietic cells, we transplanted irradiated, congenic recipients with bone marrow from tgRhoA or WT littermate mice. All recipients of tgRhoA bone marrow, but none that received WT bone marrow, developed ear and tail inflammation that began within 8 weeks of transplantation (Figure 2D; supplemental Figure 3). Ten weeks after transplant, recipients of both WT and tgRhoA bone marrow showed nearly full donor myeloid chimerism, as noted by more than 90% CD45.1$^-$CD11b$^+$ cells (Figure 2E). Consistent with defects in tgRhoA T-cell development, the proportion of donor-derived splenic CD4$^+$ T cells was significantly lower in recipients of tgRhoA bone marrow compared with recipients of WT bone

marrow (Figure 2F). In contrast, the mean proportion of donor-derived $CD4^+$ T cells recovered from tail skin of tgRhoA bone marrow recipients was increased compared with recipients of WT bone marrow (Figure 2F).

To determine whether differential T-cell activation or differentiation might contribute to this autoimmune phenotype, we further analyzed peripheral $CD4^+$ T-cell populations. TgRhoA mice between 8 and 12 weeks of age had a 25- to 30-fold reduction in absolute numbers of naive ($CD62L^+CD44^-$)[22,23] $CD4^+$ T cells in spleen compared with WT littermates, (Figure 2G). In contrast, the absolute numbers of activated ($CD62L^-CD44^+$) splenic $CD4^+$ T cells were similar in tgRhoA and WT mice, which resulted in a marked increase in the relative percentage of $CD4^+$ cells in tgRhoA mice (Figure 2G). We hypothesized that defects in regulatory T-cell (T_{reg}) differentiation might contribute to autoimmune phenotypes in tgRhoA mice. However, these mice had a significantly increased proportion of T_{reg} cells (marked by coexpression of CD25 and Foxp3[24-26]) compared with WT littermates (Figure 2G), although there was a slight decrease in absolute numbers.

Given the known role of RhoA and other small GTPases in modulating TCR signaling,[27,28] we interrogated whether RhoA G17V expression affected this pathway. To allow for antigen-specific TCR activation, we bred tgRhoA or control littermates to express the transgenic Ovalbumin specific OT-II T-cell receptor (OT-II).[29] We isolated naive $CD4^+$ T cells ($CD4^+CD62L^+CD44^-CD25^-$) and activated them with congenic irradiated splenocytes pulsed with the $Ova_{323-339}$ peptide or with the downstream activator PMA-ionomycin for 48 hours. At this point, tgRhoA-naive T cells activated by $Ova_{323-339}$ showed a significant increase in expression of the activation markers CD69 (86.4% vs 59.0%; $P < .001$) and CD25 (85.3% vs 56.9%; $P < .001$) compared with control littermates. This indicates that the threshold for TCR activation by proximal TCR signaling in naive CD4 T cells is reduced by RhoA G17V expression. This TCR-mediated hyperreactivity is consistent with a neomorphic function for RhoA G17V and contrasts with the decreased response to TCR signaling in a RhoA loss-of-function model.[30] The percentage of cells expressing CD25 induced by PMA-ionomycin was also significantly higher in tgRhoA cells (Figure 2H), suggesting there may be further effects of RhoA G17V on stimulation downstream of the TCR.

T_{FH}-cell expansion and humoral autoimmunity from RhoA G17V

The strong association between RhoA G17V mutation and T_{FH} lymphomas led us to postulate that expression of RhoA G17V in CD4 T cells might preferentially expand T_{FH} compartments or follicular regulatory T cells (T_{FR}), which can modulate T_{FH} function.[31,32] To test this hypothesis, we evaluated splenic $CD4^+$ cells from 10-week-old mice. tgRhoA mice had a 3-fold increased percentage of $CXCR5^+PD\text{-}1^+$ double-expressing cells, which mark both T_{FH} and T_{FR} cells (Figure 3A). Flow cytometric analysis of splenic $CD4^+$ cells revealed a 2-fold increase in the percentage of $CD4^+CXCR5^+PD\text{-}1^+/Foxp3^+$ cells in tgRhoA mice compared with WT littermates (supplemental Figure 4A-B). Thus, CD4-mediated expression of RhoA G17V results in relative expansion of both T_{FH} and T_{FR} populations. Expression of ICOS was also significantly increased in splenic $CD4^+$ cells from tgRhoA mice, both in comparison with WT naive T cells and to WT $CD4^+CXCR5^+PD\text{-}1^+$ cells (Figure 3A-D). We found similar results in lymph nodes harvested from these mice (supplemental Figure 5A).

We generated a transcriptional signature by comparing whole-transcriptome sequencing (RNAseq) data from purified tgRhoA activated ($CD62L^-CD44^+$) T cells and WT controls. GSEA using this signature demonstrated enrichment of a T_{FH} molecular signature compared with other CD4 effector T-cell types, including T_H1, T_H2, and T_H17 cells (supplemental Tables 1 and 2).[33]

AITL is extremely uncommon in children and young adults,[2] which raised the possibility that phenotypes from RhoA G17V would be accentuated with aging. To address this, we analyzed 30-week-old tgRhoA mice and WT controls. $CD4^+CXCR5^+PD\text{-}1^+$ cells were increased in both aged tgRhoA mice and control littermates compared with younger mice, with $CXCR5^+PD\text{-}1^+$ cells comprising 37.8% of $CD4^+$ cells in tgRhoA mice compared with 16.2% of control littermates (Figure 3E-H). Again, we found similar results in lymph nodes harvested from these mice (supplemental Figure 5B).

Plasma IgG levels were similar in tgRhoA and WT controls (Figure 3I), indicating that tgRhoA T_{FH} cells can promote differentiation of B cells to plasma cells. In fact, 30-week-old tgRhoA mice had elevated anti-double-stranded DNA titers in peripheral blood (Figure 3C), which can result in immune complex deposition in glomeruli.[34] Immunofluorescence staining of mouse IgG in kidneys demonstrated a significant increase in IgG antibody deposition in the glomeruli of 30-week-old tgRhoA mice compared with WT littermates (Figure 3J-K). These increased immunoglobulin titers were not the result of mono- or oligoclonality of plasma cell populations based on serum protein electrophoresis (supplemental Figure 6A-B). Taken together, this indicates that *Cd4*-mediated expression of RhoA G17V results in humoral autoimmunity in aged mice.

Transcriptional effects from RhoA G17V expression in CD4 T cells

To nominate pathways that mediate the phenotypes associated with RhoA G17V expression, we performed RNAseq of naive and activated $CD4^+$ populations. Principal component analysis demonstrated that differences between activation status rather than expression of RhoA G17V dominated the variance in gene sets (Figure 4A). Clustering analysis of the top 1000 variable genes showed the expected clustering of biological replicates (Figure 4B). GSEA, using the Hallmark signatures[35] from the Broad Institute MSigDB database, identified multiple mTORc1-associated signatures among the top 10 enriched among tgRhoA T cells (FDR $q < 0.0001$; Figure 4C).

The mTORc1 pathway is known to modulate T-cell activation,[36] and key components of mTORc1 and mTORc2 complexes affect T_{FH} differentiation and function.[9,10] RhoA and its yeast homolog Rho1 negatively regulate mTORc1 and its homolog TORC1, respectively.[37,38] A dominant-negative effect on RhoA signaling induced by the G17V mutation would thus be expected to promote mTORc1 signaling. We noted that a PI3K-AKT-mTOR signaling signature was also among the top 10 enriched in tgRhoA-naive CD4 T cells (Figure 4C). This is consistent with findings by Zang et al[17] and a report by Cortes et al,[39] which both identified

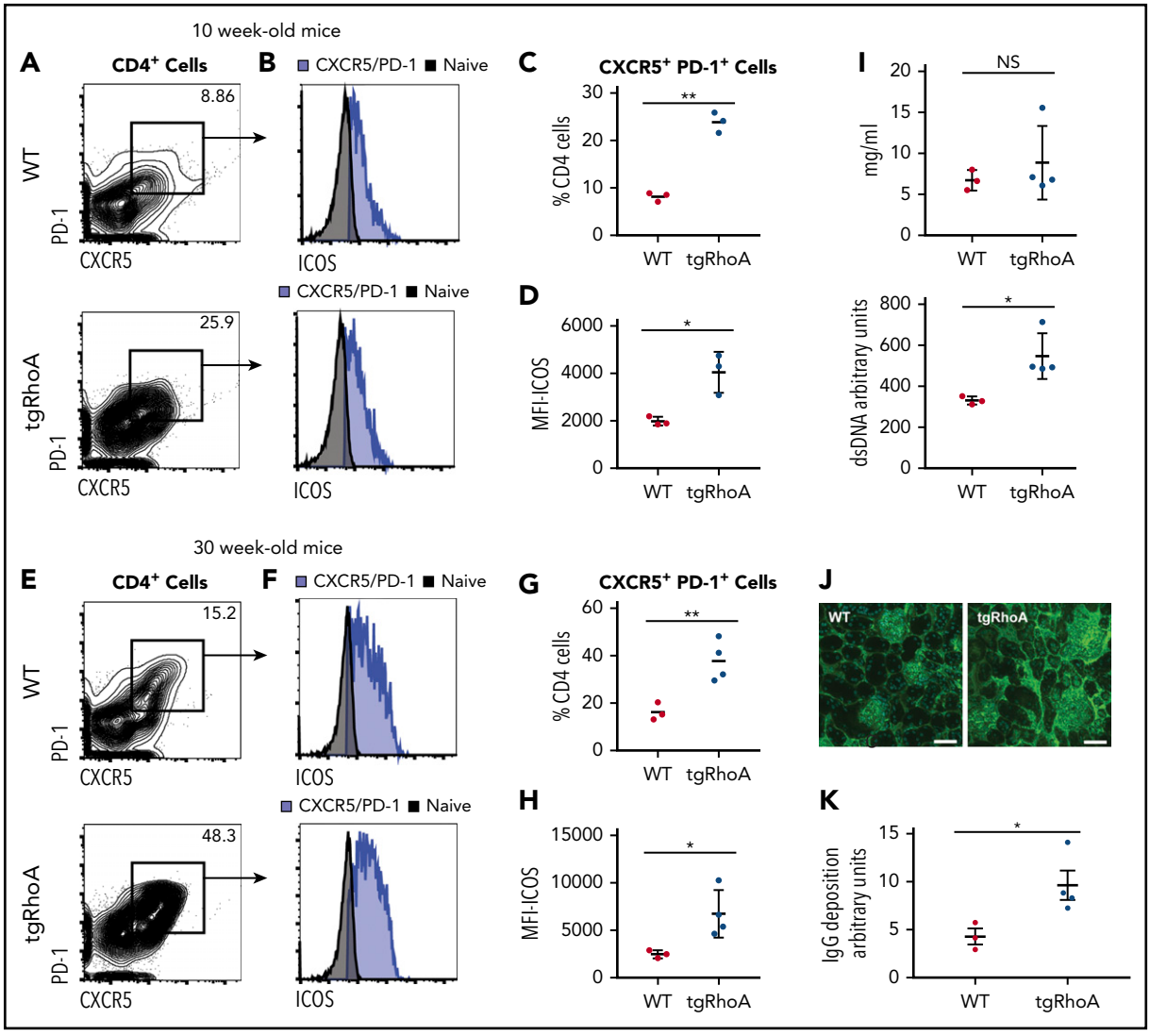

Figure 3. TgRhoA mice have increased T_{FH} compartments. (A) Splenic CD4+ cell expression of CXCR5 and PD-1 in CD4 cells from 10-week-old WT vs tgRhoA littermates. (B) ICOS expression in CD4+CXCR5+PD-1+ from WT and tgRhoA littermates. Naive CD4 T cells in both plots are from WT mice. (C) Percentage of CD4+ cells that are CXCR5+PD-1+ ($P = .0021$). (D) ICOS mean fluorescence intensity among CD4+CXCR5+PD-1+ from both genotypes ($P = .0472$). (E-H) The same approaches in (A-D) applied to 30-week -old mice. $P = .0093$ for (G). $P = .0397$ for (H). (I) ELISA of serum IgG (top, P = NS) and double-stranded DNA (bottom, $P = .0273$) from 30-week-old mice. (J) Immunofluorescence of representative glomeruli from WT or tgRhoA mice. Mouse IgG, green (Alexa 488); DAPI, blue. Scale bar, 50 μM. (K) IgG deposition from WT or tgRhoA littermates was quantified from at least 7 different sections per mouse, and the mean IgG deposition per section is shown for WT and tgRhoA (4.26 vs 9.61; $P = .0206$). All P values from t test with Welch's correction.

PI3K activation in T cells expressing RhoA G17V. Other gene sets highly enriched in tgRhoA naive T cells (allograft rejection, oxidative phosphorylation, c-MYC signaling) are consistent with heightened proliferation and metabolism in these cells.

Because of the high frequency of concurrent TET2 and RHOA G17V mutations in T_{FH}-like lymphomas, we crossed tgRhoA mice to conditional *Tet2*$^{fl/fl}$ mice[40] and induced *Tet2* deletion with the Vav-Cre transgene. This approach results in loss of *Tet2* throughout the hematopoietic compartment, and thereby recapitulates the sequence of events in patients with T_{FH}-like lymphomas. In these patients, TET2 mutations can be present within hematopoietic stem cells, but RHOA G17V develops within differentiating T cells.[13] RhoA G17V maintains many of its functional consequences when combined with *Tet2* deletion, as tgRhoA; *Tet2*$^{fl/fl}$; Vav-Cre^{+} mice developed the tail inflammation and fibrosis observed in tgRhoA mice, whereas *Tet2*$^{fl/fl}$; Vav-Cre^{+} mice showed no signs of this phenotype (supplemental Figure 7A-B).

Next, we used RNAseq to determine differential gene expression of T_{FH} cells from tgRhoA; *Tet2*$^{fl/fl}$; Vav-Cre^{+} mice compared with T_{FH} cells from *Tet2*$^{fl/fl}$; Vav-Cre^{+} mice 6 days after immunization with NP40-Ovalbumin, with alum as an adjuvant (NP40-Ova) (Figure 4A-B). We were unable to recover enough T_{FH} cells from tgRhoA mice to perform RNAseq and compare with the other populations. As observed in RhoA G17V-expressing naive T cells, GSEA using this differential analysis identified marked enrichment of the mTORc1 associated signature in T_{FH} cells from tgRhoA; *Tet2*$^{fl/fl}$; Vav-Cre^{+} mice (FDR $q < 0.0001$; Figure 4D). No enrichment of mTORc1-associated pathways was observed in the top 10 gene sets that distinguished between *Tet2*$^{fl/fl}$; Vav-Cre^{+} T_{FH} cells and WT T_{FH} cells (supplemental Figure 8). Interestingly,

enrichment of the IL2-STAT5 signaling pathway was observed in tgRhoA T_{FH} cells (Figure 4D), naive tgRhoA $CD4^+$ T cells (Figure 4C) and *Tet2*$^{fl/fl}$; Vav-Cre^+ T_{FH} cells (supplemental Figure 8) compared with their WT counterparts. This suggests that enrichment of this signature may be a nonspecific indicator of cell activation that can be affected by both RhoA G17V and Tet2 loss.

To determine whether mTORc1 signaling in tgRhoA T cells could be enhanced by proximal TCR signaling, we activated splenic naive $CD4^+$ T cells from 10-week-old mice through crosslinking of CD3 and CD28. Signaling through the proximal TCR can activate mTORc1 signaling in a Carma1- and MALT1-dependent fashion.[41] WT and tgRhoA naive $CD4^+$ T cells showed equal increases in phosphorylation of mTORc1 pathway targets S6 and 4EBP1 after 5 minutes of incubation (Figure 4E; supplemental Figure 9A). After 30 minutes of activation, tgRhoA cells showed increased phosphorylation of S6, 4EBP1, and the mTOR regulator Akt (Figure 4E; supplemental Figure 9B) compared with WT cells. Taken together, this indicates that RhoA G17V expression results in increased mTORc1 signaling that can be stimulated by proximal TCR signaling.

RhoA G17V promotes T_{FH}-like lymphomas

Tet2$^{fl/fl}$; *Vav*-Cre^+ mice can develop myeloid malignancies as early as 140 days after birth,[40,42] and mice homozygous for a hypomorphic *Tet2* mutation develop T_{FH}-like lymphomas beginning at 300 days.[43] To assess the effects of RhoA G17V on T-cell lymphomagenesis, we generated tgRhoA; *Tet2*$^{fl/fl}$; Vav-Cre^+; OT-II and *Tet2*$^{fl/fl}$; Vav-Cre^+; OT-II mice and immunized monthly with NP-40-Ova using Alum as an adjuvant. NP-40-Ova immunization of Ova-specific OT-II T cells was performed in an attempt to mimic AITL microenvironments, which almost universally harbor EBV infected B cells[44] that may provide a chronic source of T-cell stimulation.[45] Mice harboring tgRhoA had reduced median survival (205 vs 314 days; $P < .0001$; Figure 5A; supplemental Table 3). All deaths before day 270 among *Tet2*$^{fl/fl}$; Vav-Cre^+; OT-II mice were a result of myeloproliferative tumors. In contrast, at least 4 of 10 tgRhoA; *Tet2*$^{fl/fl}$; Vav-Cre^+; OT-II mice succumbed to T-cell lymphomas before day 270 ($P = .0177$; Figure 5B; supplemental Table 3).

Mice with T-cell lymphomas developed lymphadenopathy, splenomegaly, and diffuse liver infiltration by large, irregular $CD4^+$ T cells (Figure 5C; supplemental Figure 10A). High endothelial venule formation (supplemental Figure 10A), another characteristic feature of AITL, was also present. Tumor cells were $CD4^+CXCR5^+PD\text{-}1^+$ and subset $BCL6^+$ (Figure 5C; supplemental Figure 10B), similar to human T_{FH}-like lymphomas.[46] Analysis of 3 tumors with RNAseq identified somatic single nucleotide variants that were confirmed with Sanger sequencing (supplemental Figure 10C). The OT-II transgene precludes the use of TCRβ rearrangements to establish clonality. Thus, we performed PCR to detect TCR Vγ1 rearrangements from equal amounts of genomic DNA, which showed evidence of clonal restriction in these tumors (supplemental Figure 10D). In addition, we observed the spontaneous development of grossly enlarged lymph nodes and spleens in 2 tgRhoA; *Tet2*$^{fl/fl}$; CD4-Cre^+ mice at 12 and 23 months of age with histology and immunophenotypic findings consistent with T-cell transformation (supplemental Figure 11A-D). Together, these data indicate that RhoA G17V expression in $CD4^+$ cells promotes the development of T_{FH}-like lymphomas in conjunction with *Tet2* loss.

Approximately 300 000 tumor cells from a tgRhoA; *Tet2*$^{fl/fl}$; Vav-Cre^+; OT-II mouse were transplanted into Nod.SCID.IL2rγ$^{-/-}$ mice. All recipients were euthanized because of progressive lymphoma within less than 28 days after transplant (Figure 5D, 5E). Interestingly, tumor cells were not detectable within 180 days or more after transplantation into either WT or TCRβ-knockout mice.

Differential gene expression analysis comparing sorted $CD4^+$ $CXCR5^+PD\text{-}1^+$ tumor cells from tgRhoA;*Tet2*$^{fl/fl}$; Vav-Cre^+; OT-II mice with *Tet2*$^{fl/fl}$; Vav-Cre^+ T_{FH} cells using GSEA of Hallmark gene sets again demonstrated enrichment of gene sets reflecting mTORc1 activity in multiple tumors (Figure 5F; supplemental Figure 12A-C). These tumors also demonstrated enrichment of GSEA signatures associated with T_{FH} cells[47,48] (supplemental Figure 13A), showed evidence of homogenous Bcl6 and ICOS expression, and did not express Foxp3 (supplemental Figure 13B-D).

Given the increased mTORc1 activity present in these cells, we tested the activity of the mTOR inhibitor everolimus[49] in Nod.SCID.IL2rγ$^{-/-}$ mice transplanted with tgRhoA; *Tet2*$^{fl/fl}$; Vav-Cre^+; OT-II lymphoma cells. After 5 days of treatment, everolimus-treated mice had significantly decreased spleen size and percent $CD4^+$ cells in the spleen compared with vehicle-treated controls (Figure 6A-B). In fact, splenic involvement was reduced in everolimus-treated mice compared with mice euthanized before treatment, indicating that treatment with everolimus reduces lymphoma involvement (Figure 6B-C). Tumor cells from everolimus-treated mice showed significantly decreased phosphorylation of S6, 4EBP1, and Akt compared with vehicle-treated controls (Figure 6D-G) consistent with an on-target effect for everolimus. Finally, we treated a separate cohort of mice transplanted with tgRhoA; *Tet2*$^{fl/fl}$; Vav-Cre^+; OT-II lymphoma cells for 21 days beginning 14 days after injection. Treatment with everolimus markedly improved overall survival compared with vehicle that extended for 12 days after drug cessation (Figure 6H).

Discussion

Our study demonstrates that *Cd4*-mediated expression of RhoA G17V is sufficient to dysregulate T-cell development and confer autoimmunity. The thymic developmental block in tgRhoA mice occurs at the transition between the $CD69^+TCR\beta^{lo}$ and $CD69^+$ $TCR\beta^{hi}$ stages, which suggests that at least some degree of positive selection has occurred.[20] We also noted increased expression of PD-1 in the $CD69^+TCR\beta^{hi}$ and $CD69^-TCR\beta^{hi}$ populations. On the basis of previous studies, this would be consistent with an increased rate of negative selection,[50] although experiments using transgenic TCR constructs that enforce negative selection would be necessary to fully confirm such a model. TCR hyperreactivity resulting from RhoA G17V expression could promote this negative selection in the thymus and underlie the increased proportion of T_{reg} and T_{FR} cells observed in tgRhoA mice. In the periphery, this hyperreactivity likely contributes to the autoreactive phenotypes we observe and possibly further depletes the naive T-cell compartment through aberrant activation of these cells.

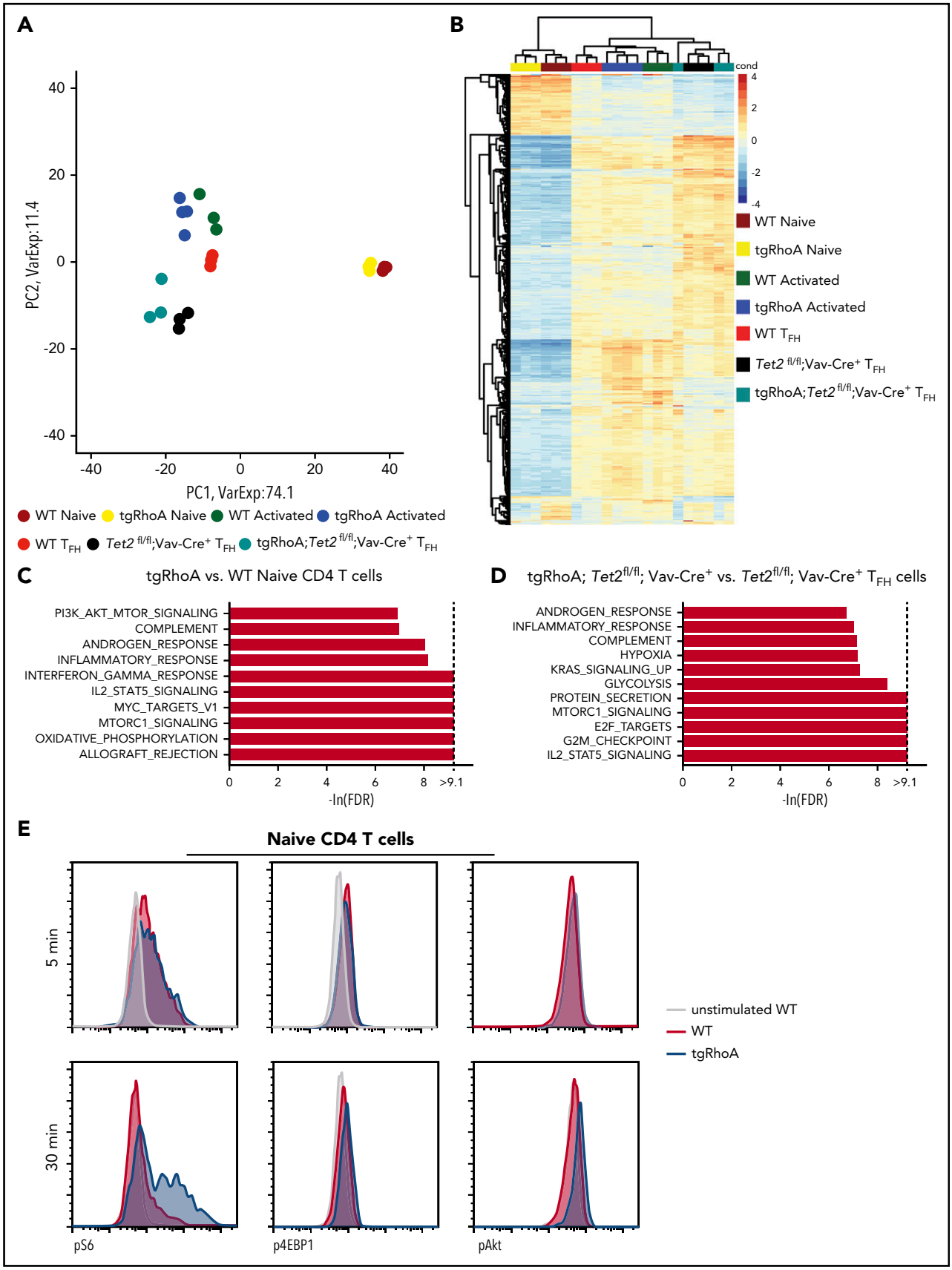

Figure 4. TgRhoA CD4 populations have transcriptional and biochemical evidence of mTORc1 pathway activation. (A) Principal component analysis of biological replicates of WT and tgRhoA CD4$^+$ naive and activated populations compared with WT, *Tet2*-deleted (Tet2) and tgRhoA; *Tet2*$^{fl/fl}$; Vav-Cre T_{FH}-cell populations 6 days after immunization with NP40-Ova/Alum. (B) Unsupervised hierarchical clustering of the same populations based on top 1000 genes. (C) Top 10 signatures enriched in tgRhoA vs WT

An alternative, although not mutually exclusive, possibility is that RhoA G17V-mediated alterations in cytoskeletal function influence differentiation by altering fundamental processes within T cells, including synapse formation, cellular polarization, or cellular migration. Additional studies will be required to determine which of these mechanisms contributes to the phenotypes observed in RhoA G17V-mutated T cells.

Our finding that the CD4 compartment is already skewed toward T_{FH} differentiation in young mice suggests there is either a bias in effector cell differentiation or that T_{FH} cells preferentially expand in the periphery compared with other effector cell populations at a very early age. The finding that this compartment is further expanded in aged mice indicates that expression of RhoA G17V supports the survival and/or differentiation of these cells. Both findings are consistent with clinical data from patients with PTCL showing an almost absolute association between RhoA G17V mutation and T_{FH}-like gene expression and immunophenotype.[51,52] Although T_{FR} cells are relatively expanded in tgRhoA mice, they do not abrogate autoimmunity induced by T_{FH} cells or lymphomagenesis, raising the possibility that these cells may be functionally defective. Alternatively, RhoA G17V expressing T_{FH} cells may overcome suppressive signaling from T_{FR} cells.

The autoimmunity observed in tgRhoA mice could result from a combination of factors, including the observed TCR hyperreactivity, changes in the polarization of tgRhoA CD4 T cells, and/or dysfunctional regulatory hematopoietic cell populations that result from transgene expression. Experiments to address the relative contributions of each of these factors are warranted to explore whether and how RhoA G17V mutation promotes autoimmunity in patients.

In combination with *Tet2* deletion, *Cd4*-mediated expression of RhoA G17V led to T-cell transformation before 10 months of age. In previous studies, mice carrying homozygous *Tet2* hypomorphic mutations or complete loss of *Tet2* combined with DNMT3A R882H mutation developed mature T-cell tumors, but only after 1 year or more.[43,53] We used a transgenic TCR and stimulated with NP40-Ova, so a direct comparison in latency between our model and previous studies is problematic. The presence of the transgenic TCR precluded use of TCRβ sequencing platforms to establish clonality of the tumors; however, we showed clonal restriction based on Vγ1 rearrangements.

Our tumors required immunocompromised hosts for propagation and did not engraft into TCRβ-deficient mice. This is possibly a result of the presence of TCRγδ cells and/or NK cells within TCRβ-deficient (but not Nod.SCID.IL2rγ$^{-/-}$) mice that mediate rejection of the tumor cells. Further studies are required to investigate which components of host immunity underlie this finding. Nonetheless, our findings that RhoA G17V increases the frequency of T-cell lymphomas and reduces latency confirms its role as a T-cell lymphoma oncogene and indicates that cellular or molecular aberrancies arising as a result of this mutation underlie key checkpoints in the progression of lymphomagenesis.

We observed enrichment of mTORc1-associated gene expression in both RhoA G17V expressing nonmalignant and T-cell tumor cells. We also demonstrated evidence of increased mTORc1 signaling after proximal TCR stimulation with an agonistic costimulatory signal. This is highly concordant with the finding from Zang et al.[17] that RhoA G17V/Tet2-deficient T cells have perturbed FoxO1 expression, phosphorylation, and subcellular localization, as FoxO1 is a negative regulator of mTORc1 signaling.[54] Similarly, Cortes et al.[39] recently described a RhoA G17V knock-in model and reported that RhoA G17V increases PI3K-mTORc1 signaling in CD4 T cells through ICOS.[39] Thus, there are now 3 independent models using distinct approaches (adoptive transfer, knock-in, and germ line transgene) that all identify aspects of PI3K-mTOR signaling induced by RhoA G17V. It will be essential to determine whether RhoA G17V mutation in patient AITLs confers a signature similar to the ones observed in these model systems. Of note, mTORc1 activity is essential for T_H17 cell differentiation, as we observed in the inflamed tails of tgRhoA mice, because deletion of Raptor (the defining subunit of the mTORc1 complex) in T cells abrogates development of this population.[55]

The role of mTORc1 in T_{FH} cell production remains unclear, as a recent report indicates that T_{FH} cells in Peyer's Patches are significantly reduced in the absence of Raptor or Rictor (the defining subunit of the mTORc2 complex), using OX40-Cre-targeted deletion of these genes.[10] In contrast, a previous publication reported an increase in T_{FH} differentiation when Raptor expression was knocked down using shRNA, whereas Rictor knockdown had minimal effect.[9] Thus, mTORc1 activity may in some contexts partially inhibit T_{FH} differentiation, whereas its ongoing activity is necessary for proliferation of these cells once fully differentiated.

Our study indicates that everolimus can inhibit the proliferation of RhoA G17V-mutated lymphomas, and it possibly exerts cytotoxic effects (Figure 6A-C). To our knowledge, only 1 previous study tested everolimus in patients with T-cell lymphomas, and that study enrolled only a single patient with T_{FH}-like lymphoma.[56] Cortes et al similarly reported that the PI3K-δγ inhibitor Duvelisib was effective in their RhoA G17V-driven lymphomas,[39] suggesting that multiple nodes within the PI3K-mTOR pathway may be targetable. Of note, we recently reported a higher than 50% response rate among patients with peripheral T-cell lymphomas to single-agent Duvelisib, including 2 of 3 (1 complete response, 1 partial response) patients with AITL.[57] Unfortunately, *RHOA* genotyping was not performed in these cases, but an ongoing trial of Duvelisib in combination with either romidepsin or bortezomib (NCT02783625) will include genotyping.

There are notable differences between our findings and those of Zang et al.[17] Transgenic RhoA G17V expression was sufficient to induce lymphopenia and autoimmunity in our mice. Unlike Zang et al.,[17] our mice also had increased percentages of Foxp3-expressing cells, including T_{reg} and T_{FR} cells. In addition, our tgRhoA mice demonstrated a relative expansion of T_{FH} cells independent of *Tet2* mutation. Our tgRhoA; *Tet2*$^{fl/fl}$; Vav-Cre^{+}

Figure 4 (continued) naive or (D) tgRhoA; *Tet2*$^{fl/fl}$; Vav-Cre^{+} vs *Tet2*$^{fl/fl}$; Vav-Cre^{+} T_{FH} cells, using Hallmark GSEA gene sets. Gene sets are ranked by normalized enrichment score values. (E) Representative flow cytometric intracellular staining of phospho-S6 (pS6), phospho-4EBP1 (p4EBP1), and phospho-Akt (pAkt) in splenic WT or tgRhoA naive CD4 T cells after CD3 and CD28 cross-linking for the indicated durations. All histograms display frequency of events as percentage of cells within the population indicated.

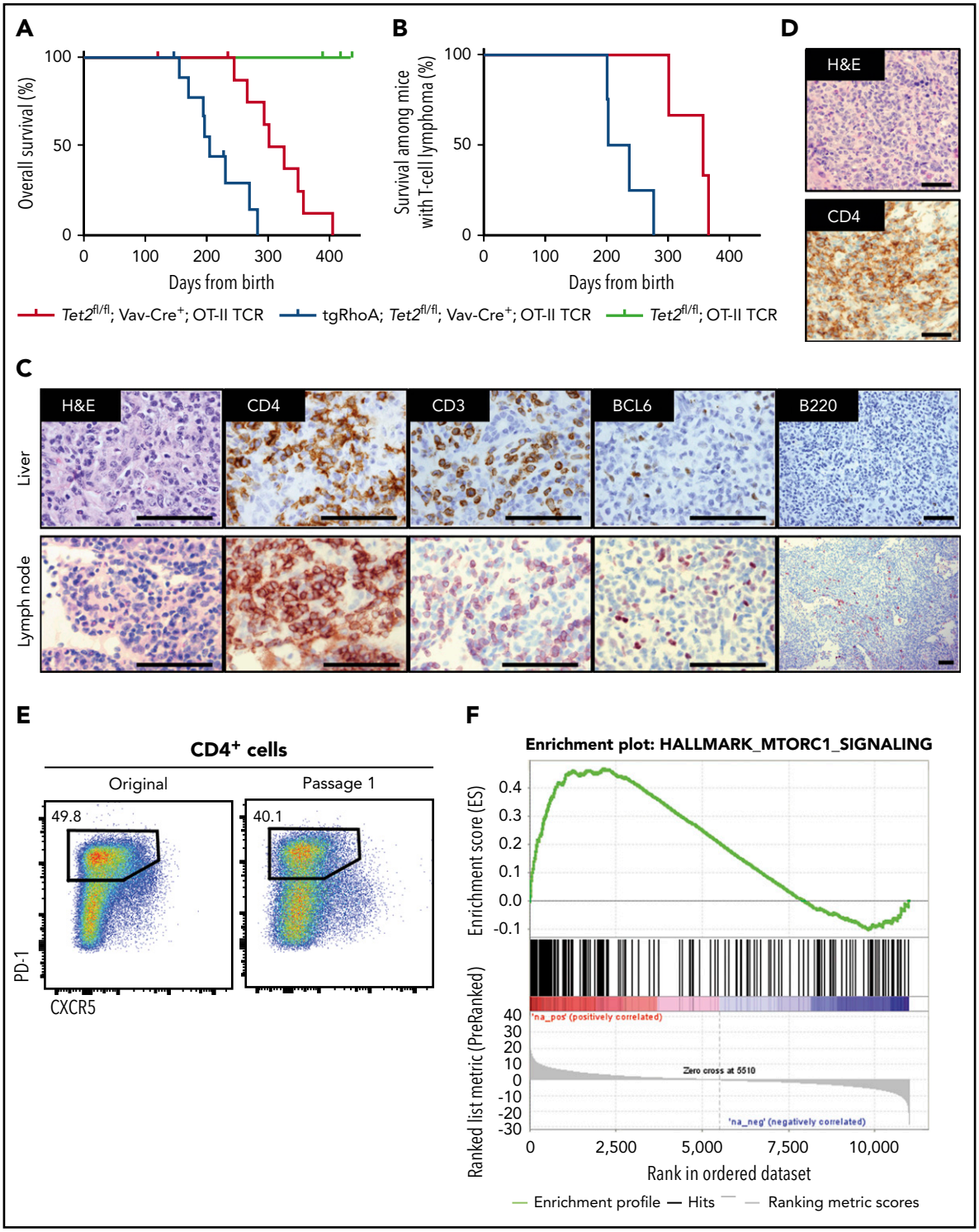

Figure 5. *Cd4*-RhoA G17V promotes T-cell transformation in concert with Tet2 loss. (A) Overall survival from birth for *Tet2*$^{fl/fl}$; Vav-Cre^{+}; OT-II (red, n = 10), tgRhoA; *Tet2*$^{fl/fl}$; Vav-Cre^{+}; OT-II (blue, n = 10), or *Tet2*$^{fl/fl}$; OT-II (green, n = 4) mice. Mice were immunized monthly with NP40-Ovalbumin, using alum as an adjuvant for up to 7 injections. One mouse from *Tet2*$^{fl/fl}$; Vav-Cre^{+}; OT-II and 1 mouse from tgRhoA; *Tet2*$^{fl/fl}$; Vav-Cre^{+}; OT-II cohorts were found dead and could not be analyzed. $P < .0001$ by Mantel-Cox test. (B) Survival of *Tet2*$^{fl/fl}$; Vav-Cre^{+}; OT-II (red, n = 3) or tgRhoA; *Tet2*$^{fl/fl}$; Vav-Cre^{+}; OT-II (blue, n = 4) mice that were confirmed to have developed T-cell tumors. $P = .0177$ by Mantel-Cox test. (C) Immunohistochemistry of tgRhoA; *Tet2*$^{fl/fl}$; Vav-Cre^{+}; OT-II lymphoma from a mouse that required euthanasia 231 days after birth showing T-cell infiltrate of lymph node and liver with markers as noted. Scale bars, 100 μM. Images taken at ×1000 except for B220 at ×200. (D) Immunohistochemical analysis of the spleen from a mouse transplanted with T-cell tumor 1 from tgRhoA; *Tet2*$^{fl/fl}$; Vav-Cre^{+}; OT-II donor. Scale bars, 100 μM. Images taken at ×400. (E) Flow cytometric analysis of CD4^{+} tumor cells from primary tgRhoA; *Tet2*$^{fl/fl}$; Vav-Cre^{+}; OT-II mouse and from secondary recipient. (F) GSEA of Hallmark mTORc1 gene set compared with *Tet2*$^{fl/fl}$; Vav-Cre^{+}; OT-II T_{FH} cells (FDR $q = 0.001125$).

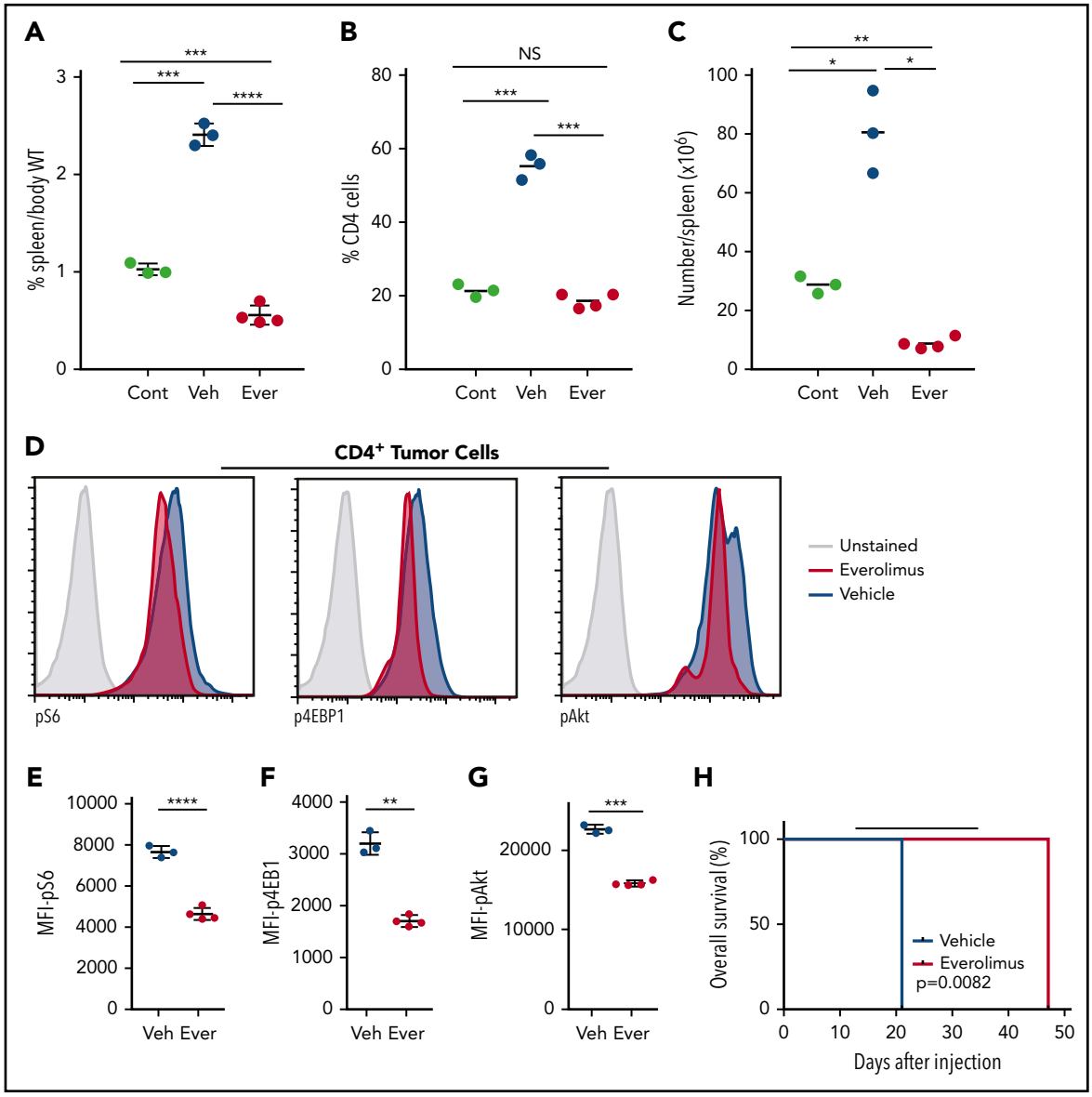

Figure 6. Everolimus suppresses mTOR signaling and improves survival in mice transplanted with tgRhoA; *Tet2*-deleted tumor cells. (A) Spleen weight as percentage body weight in Nod.SCID.IL2rγ$^{-/-}$ mice. Control (Cont) mice were euthanized 14 days after injection with 500 000 cells from tumor 1. The remainder of the cohort was dosed with daily gavage of 10 mg/kg Everolimus (Ever) or vehicle (Veh) daily for 5 consecutive days until they were euthanized for analysis 2 hours after the final dose. Quantification of the percentage (B) or absolute number (C) of CD4$^+$ cells present in the spleens of mice. (D) Intracellular flow cytometric analysis of pAkt and mTORc1 signaling components pS6 and p4EBP1 in splenic CD4$^+$ cells from everolimus-treated (red) or vehicle-treated (blue) mice. Control peaks are from unstained vehicle CD4$^+$ cells. All histograms display frequency of events as percentage of cells within the population indicated. (E-G) Mean fluorescence intensity from replicates of indicated phosphoproteins. All *P* values from *t* test with Welch's correction. (H) Overall survival of recipients of tgRhoA; *Tet2*$^{fl/fl}$; Vav-Cre$^+$; OT-II tumor cells treated with either daily oral gavage of 10 mg/kg everolimus or vehicle from days 14 to 34 (indicated by black bar) after transfer. Each group consisted of 4 mice. *P* value from Mantel-Cox test.

mice also generated tumors, which could result from differences in transgene dosage and/or stimulation with NP40-Ova. By expressing a germ line transgene, we ensured that all CD4-expressing cells contained the RhoA G17V construct, which overcomes concerns that transduction may bias toward specific T-cell populations.

The stages of T-cell differentiation in humans at which RhoA G17V mutation occur are currently not known. If the mutations occur within more differentiated CD4$^+$ cells (eg, effector or memory CD4$^+$ cells), some of the phenotypes we observe may not be clinically relevant. In contrast, it is possible that patients who present with lymphopenia and/or autoimmunity may have developed the mutation at an earlier stage of CD4 T-cell differentiation, and thus manifest similar phenotypes to our mice.

In conclusion, expression of RhoA G17V in murine CD4$^+$ cells has dual effects both by contributing to CD4 T-cell autonomous transformation and by promoting immune dysregulation that results in autoimmunity. Studies of patients with T_{FH}-like lymphomas are needed to determine whether specific aspects of immune dysregulation, including rash, autoimmune hemolytic anemia, immune thrombocytopenia, and hypergammaglobulinemia,[2,3] also result from the expression of RhoA G17V in nonmalignant cells. Finally,

the identification of additional aberrancies that fully transform T cells in conjunction with RhoA G17V and *Tet2* loss, as well as the vulnerabilities induced by these aberrancies, are now feasible.

Acknowledgments

The authors are grateful to Koichi Oshima for assistance with histological interpretation and preparation of mouse tumor slides, and also would like to thank Hye-Jung Kim, Harvey Cantor, Peter Sage, Arlene Sharpe, Zhuting Hu, and Petr Jarolim for their generous technical assistance in these studies. S.Y.N. is supported by an American Cancer Society–Kirby Foundation Postdoctoral Fellowship PF-16-149-01-TBG, a Harvard Medical School CMeRIT Award, and Conquer Cancer Foundation of ASCO Young Investigator Award 11489. This work is also supported by a Leukemia and Lymphoma Society Specialized Center of Research award (D.M.W. and J.C.A.).

Authorship

Contribution: S.Y.N. designed, executed, and analyzed the experiments; L.B. and T.d.S. assisted in performing the experiments; K.S., J.C.A., and A.L. assisted with analysis; D.M.W. designed and analyzed the experiments; and S.Y.N. and D.M.W. cowrote the manuscript.

Conflict-of-interest disclosure: D.M.W. is a paid consultant and receives research support from Novartis. The remaining authors declare no competing financial interests.

Correspondence: David M. Weinstock, Dana-Farber Cancer Institute, 450 Brookline Ave, Dana 510B, Boston, MA 02215; e-mail: dweinstock@partners.org.

Footnotes

Submitted 26 November 2017; accepted 7 May 2018. Prepublished online as *Blood* First Edition paper, 16 May 2018; DOI 10.1182/blood-2017-11-818617.

The online version of this article contains a data supplement.

The publication costs of this article were defrayed in part by page charge payment. Therefore, and solely to indicate this fact, this article is hereby marked "advertisement" in accordance with 18 USC section 1734.

REFERENCES

1. Swerdlow SH, Campo E, Pileri SA, et al. The 2016 revision of the World Health Organization classification of lymphoid neoplasms. *Blood*. 2016;127(20):2375-2390.
2. Federico M, Rudiger T, Bellei M, et al. Clinicopathologic characteristics of angioimmunoblastic T-cell lymphoma: analysis of the international peripheral T-cell lymphoma project. *J Clin Oncol*. 2013;31(2):240-246.
3. Mourad N, Mounier N, Brière J, et al; Groupe d'Etude des Lymphomes de l'Adulte. Clinical, biologic, and pathologic features in 157 patients with angioimmunoblastic T-cell lymphoma treated within the Groupe d'Etude des Lymphomes de l'Adulte (GELA) trials. *Blood*. 2008;111(9):4463-4470.
4. de Leval L, Rickman DS, Thielen C, et al. The gene expression profile of nodal peripheral T-cell lymphoma demonstrates a molecular link between angioimmunoblastic T-cell lymphoma (AITL) and follicular helper T (TFH) cells. *Blood*. 2007;109(11):4952-4963.
5. Vinuesa CG, Linterman MA, Yu D, MacLennan IC. Follicular helper T cells. *Annu Rev Immunol*. 2016;34(1):335-368.
6. Dorfman DM, Brown JA, Shahsafaei A, Freeman GJ. Programmed death-1 (PD-1) is a marker of germinal center-associated T cells and angioimmunoblastic T-cell lymphoma. *Am J Surg Pathol*. 2006;30(7):802-810.
7. Haynes NM, Allen CD, Lesley R, Ansel KM, Killeen N, Cyster JG. Role of CXCR5 and CCR7 in follicular Th cell positioning and appearance of a programmed cell death gene-1high germinal center-associated subpopulation. *J Immunol*. 2007;179(8):5099-5108.
8. Choi YS, Kageyama R, Eto D, et al. ICOS receptor instructs T follicular helper cell versus effector cell differentiation via induction of the transcriptional repressor Bcl6. *Immunity*. 2011;34(6):932-946.
9. Ray JP, Staron MM, Shyer JA, et al. The interleukin-2-mTORc1 kinase axis defines the signaling, differentiation, and metabolism of T helper 1 and follicular B helper T cells. *Immunity*. 2015;43(4):690-702.
10. Zeng H, Cohen S, Guy C, et al. mTORC1 and mTORC2 kinase signaling and glucose metabolism drive follicular helper T cell differentiation. *Immunity*. 2016;45(3):540-554.
11. Couronné L, Bastard C, Bernard OA. TET2 and DNMT3A mutations in human T-cell lymphoma. *N Engl J Med*. 2012;366(1):95-96.
12. Odejide O, Weigert O, Lane AA, et al. A targeted mutational landscape of angioimmunoblastic T-cell lymphoma. *Blood*. 2014;123(9):1293-1296.
13. Sakata-Yanagimoto M, Enami T, Yoshida K, et al. Somatic RHOA mutation in angioimmunoblastic T cell lymphoma. *Nat Genet*. 2014;46(2):171-175.
14. Palomero T, Couronné L, Khiabanian H, et al. Recurrent mutations in epigenetic regulators, RHOA and FYN kinase in peripheral T cell lymphomas. *Nat Genet*. 2014;46(2):166-170.
15. Yoo HY, Sung MK, Lee SH, et al. A recurrent inactivating mutation in RHOA GTPase in angioimmunoblastic T cell lymphoma. *Nat Genet*. 2014;46(4):371-375.
16. Rougerie P, Delon J. Rho GTPases: masters of T lymphocyte migration and activation. *Immunol Lett*. 2012;142(1-2):1-13.
17. Zang S, Li J, Yang H, et al. Mutations in 5-methylcytosine oxidase TET2 and RhoA cooperatively disrupt T cell homeostasis. *J Clin Invest*. 2017;127(8):2998-3012.
18. Sawada S, Scarborough JD, Killeen N, Littman DR. A lineage-specific transcriptional silencer regulates CD4 gene expression during T lymphocyte development. *Cell*. 1994;77(6):917-929.
19. Zampell JC, Yan A, Elhadad S, Avraham T, Weitman E, Mehrara BJ. CD4(+) cells regulate fibrosis and lymphangiogenesis in response to lymphatic fluid stasis. *PLoS One*. 2012;7(11):e49940.
20. Yamashita I, Nagata T, Tada T, Nakayama T. CD69 cell surface expression identifies developing thymocytes which audition for T cell antigen receptor-mediated positive selection. *Int Immunol*. 1993;5(9):1139-1150.
21. Nurieva R, Yang XO, Martinez G, et al. Essential autocrine regulation by IL-21 in the generation of inflammatory T cells. *Nature*. 2007;448(7152):480-483.
22. Weinberg AD, English M, Swain SL. Distinct regulation of lymphokine production is found in fresh versus in vitro primed murine helper T cells. *J Immunol*. 1990;144(5):1800-1807.
23. Powers GD, Abbas AK, Miller RA. Frequencies of IL-2- and IL-4-secreting T cells in naive and antigen-stimulated lymphocyte populations. *J Immunol*. 1988;140(10):3352-3357.
24. Hori S, Nomura T, Sakaguchi S. Control of regulatory T cell development by the transcription factor Foxp3. *Science*. 2003;299(5609):1057-1061.
25. Khattri R, Cox T, Yasayko SA, Ramsdell F. An essential role for Scurfin in CD4+CD25+ T regulatory cells. *Nat Immunol*. 2003;4(4):337-342.
26. Fontenot JD, Gavin MA, Rudensky AY. Foxp3 programs the development and function of CD4+CD25+ regulatory T cells. *Nat Immunol*. 2003;4(4):330-336.
27. Corre I, Gomez M, Vielkind S, Cantrell DA. Analysis of thymocyte development reveals that the GTPase RhoA is a positive regulator of T cell receptor responses in vivo. *J Exp Med*. 2001;194(7):903-914.
28. Guo F, Hildeman D, Tripathi P, Velu CS, Grimes HL, Zheng Y. Coordination of IL-7 receptor and T-cell receptor signaling by cell-division cycle 42 in T-cell homeostasis. *Proc Natl Acad Sci USA*. 2010;107(43):18505-18510.
29. Robertson JM, Jensen PE, Evavold BD. DO11.10 and OT-II T cells recognize a C-terminal ovalbumin 323-339 epitope. *J Immunol*. 2000;164(9):4706-4712.
30. Yang JQ, Kalim KW, Li Y, et al. RhoA orchestrates glycolysis for TH2 cell differentiation and allergic airway inflammation. *J Allergy Clin Immunol*. 2016;137(1):231-245.

31. Linterman MA, Pierson W, Lee SK, et al. Foxp3+ follicular regulatory T cells control the germinal center response. *Nat Med*. 2011; 17(8):975-982.

32. Chung Y, Tanaka S, Chu F, et al. Follicular regulatory T cells expressing Foxp3 and Bcl-6 suppress germinal center reactions. *Nat Med*. 2011;17(8):983-988.

33. Nurieva RI, Chung Y, Hwang D, et al. Generation of T follicular helper cells is mediated by interleukin-21 but independent of T helper 1, 2, or 17 cell lineages. *Immunity*. 2008;29(1):138-149.

34. Kim HJ, Verbinnen B, Tang X, Lu L, Cantor H. Inhibition of follicular T-helper cells by CD8(+) regulatory T cells is essential for self tolerance. *Nature*. 2010;467(7313):328-332.

35. Liberzon A, Birger C, Thorvaldsdóttir H, Ghandi M, Mesirov JP, Tamayo P. The Molecular Signatures Database (MSigDB) hallmark gene set collection. *Cell Syst*. 2015;1(6): 417-425.

36. Powell JD, Delgoffe GM. The mammalian target of rapamycin: linking T cell differentiation, function, and metabolism. *Immunity*. 2010;33(3):301-311.

37. Yan G, Lai Y, Jiang Y. The TOR complex 1 is a direct target of Rho1 GTPase. *Mol Cell*. 2012; 45(6):743-753.

38. Gordon BS, Kazi AA, Coleman CS, et al. RhoA modulates signaling through the mechanistic target of rapamycin complex 1 (mTORC1) in mammalian cells. *Cell Signal*. 2014;26(3): 461-467.

39. Cortes JR, Ambesi-Impiombato A, Couronne L, et al. RHOA G17V induces T follicular helper cell specification and promotes lymphomagenesis. *Cancer Cell*. 2018;33(2):259-273.

40. Moran-Crusio K, Reavie L, Shih A, et al. Tet2 loss leads to increased hematopoietic stem cell self-renewal and myeloid transformation. *Cancer Cell*. 2011;20(1):11-24.

41. Hamilton KS, Phong B, Corey C, et al. T cell receptor-dependent activation of mTOR signaling in T cells is mediated by Carma1 and MALT1, but not Bcl10. *Sci Signal*. 2014;7(329):ra55.

42. Quivoron C, Couronné L, Della Valle V, et al. TET2 inactivation results in pleiotropic hematopoietic abnormalities in mouse and is a recurrent event during human lymphomagenesis. *Cancer Cell*. 2011;20(1):25-38.

43. Muto H, Sakata-Yanagimoto M, Nagae G, et al. Reduced TET2 function leads to T-cell lymphoma with follicular helper T-cell-like features in mice. *Blood Cancer J*. 2014;4(12): e264.

44. Weiss LM, Jaffe ES, Liu XF, Chen YY, Shibata D, Medeiros LJ. Detection and localization of Epstein-Barr viral genomes in angioimmunoblastic lymphadenopathy and angioimmunoblastic lymphadenopathy-like lymphoma. *Blood*. 1992;79(7):1789-1795.

45. Dunleavy K, Wilson WH, Jaffe ES. Angioimmunoblastic T cell lymphoma: pathobiological insights and clinical implications. *Curr Opin Hematol*. 2007;14(4):348-353.

46. Swerdlow SHCE, Harris NL, Jaffe ES, et al. WHO Classification of Tumours of Haematopoietic and Lymphoid Tissues. Lyon, France: International Agency for Research on Cancer; 2008.

47. Hale JS, Youngblood B, Latner DR, et al. Distinct memory CD4+ T cells with commitment to T follicular helper- and T helper 1-cell lineages are generated after acute viral infection. *Immunity*. 2013;38(4):805-817.

48. Liu X, Yan X, Zhong B, et al. Bcl6 expression specifies the T follicular helper cell program in vivo. *J Exp Med*. 2012;209(10):1841-1852.

49. Boulay A, Zumstein-Mecker S, Stephan C, et al. Antitumor efficacy of intermittent treatment schedules with the rapamycin derivative RAD001 correlates with prolonged inactivation of ribosomal protein S6 kinase 1 in peripheral blood mononuclear cells. *Cancer Res*. 2004;64(1):252-261.

50. Daley SR, Hu DY, Goodnow CC. Helios marks strongly autoreactive CD4+ T cells in two major waves of thymic deletion distinguished by induction of PD-1 or NF-κB. *J Exp Med*. 2013;210(2):269-285.

51. Manso R, Sánchez-Beato M, Monsalvo S, et al. The RHOA G17V gene mutation occurs frequently in peripheral T-cell lymphoma and is associated with a characteristic molecular signature. *Blood*. 2014;123(18):2893-2894.

52. Ondrejka SL, Grzywacz B, Bodo J, et al. Angioimmunoblastic T-cell lymphomas with the RHOA p.Gly17Val mutation have classic clinical and pathologic features. *Am J Surg Pathol*. 2016;40(3):335-341.

53. Scourzic L, Couronné L, Pedersen MT, et al. DNMT3A(R882H) mutant and Tet2 inactivation cooperate in the deregulation of DNA methylation control to induce lymphoid malignancies in mice. *Leukemia*. 2016;30(6): 1388-1398.

54. Chen CC, Jeon SM, Bhaskar PT, et al. FoxOs inhibit mTORC1 and activate Akt by inducing the expression of Sestrin3 and Rictor. *Dev Cell*. 2010;18(4):592-604.

55. Delgoffe GM, Pollizzi KN, Waickman AT, et al. The kinase mTOR regulates the differentiation of helper T cells through the selective activation of signaling by mTORC1 and mTORC2. *Nat Immunol*. 2011;12(4):295-303.

56. Witzig TE, Reeder C, Han JJ, et al. The mTORC1 inhibitor everolimus has antitumor activity in vitro and produces tumor responses in patients with relapsed T-cell lymphoma. *Blood*. 2015;126(3):328-335.

57. Horwitz SM, Koch R, Porcu P, et al. Activity of the PI3K-δ,γ inhibitor duvelisib in a phase 1 trial and preclinical models of T-cell lymphoma. *Blood*. 2018;131(8):888-898.